Dual fluorescence and fast intramolecular charge transfer with 4-(diisopropylamino)benzonitrile in alkane solvents

Attila Demeter [a,1], Sergey Druzhinin [a], Mathew George [a], Edwin Haselbach [b], Jean-Luc Roulin [b], Klaas A. Zachariasse [a,*]

[a] *Max-Planck-Institut für biophysikalische Chemie, Spektroskopie und Photochemische Kinetik, D-37070 Göttingen, Germany*
[b] *Institut für Physikalische Chemie, Universität Fribourg, Perolles, CH-1700 Fribourg, Switzerland*

Received 17 April 2000

Abstract

Dual fluorescence and fast intramolecular charge transfer (ICT) is observed with 4-(diisopropylamino)benzonitrile (DIABN) in alkane solvents. The rate constant k_a for the reaction from the locally excited (LE) to the ICT state has a value of 3.4×10^{11} s^{-1} in *n*-hexane at 25°C, with an activation energy E_a of 6 kJ mol^{-1}. Efficient intersystem crossing with a yield of 0.94 takes place from the ICT state. With 4-(dimethylamino)benzonitrile, in contrast, dual fluorescence is not observed in alkanes. The charge transfer reaction of DIABN is mainly favoured by its small energy gap $\Delta E(S_1, S_2)$, in accordance with the PICT model for ICT in aminobenzonitriles. © 2000 Elsevier Science B.V. All rights reserved.

1. Introduction

The changes in molecular structure taking place in 4-(dimethylamino)benzonitrile (DMABN) and its dual fluorescent derivatives during the reaction from the initially prepared locally excited (LE) to the intramolecular charge transfer (ICT) state are the subject of continuing investigation [1–6]. In the *twisted ICT* (TICT) model [7,8], it is postulated that the dimethylamino group of DMABN undergoes a twist of 90° relative to the benzonitrile moiety, from a coplanar configuration in LE to a perpendicular structure in the ICT state. The *planar ICT* (PICT) model [2,4,9,10], on the other hand, assumes that the ICT state of DMABN is largely planar, whereas its dimethylamino group in the LE state is considered to have retained at least part of the pyramidal configuration present in the ground state [11,12]. In the PICT model the magnitude of the energy gap $\Delta E(S_1, S_2)$ between the two lowest excited singlet states plays a crucial role [2]. The importance of the planarisation of the amino nitrogen during the LE → ICT reaction has been deduced from the strong reduction in the efficiency of the ICT reaction in the series of heterocyclic 4-aminobenzonitriles PnC when the ring size n of the amino substituent decreases from 8 to 3 [9,10,13]. For heterocyclic

---

* Corresponding author. Fax: +49-551-201-1501; e-mail: kzachar@gwdg.de

[1] On leave from the Institute of Chemistry, Chemical Research Center, Hungarian Academy of Sciences. P.O. Box 17, 1525 Budapest, Hungary.

amines, the energy required for planarisation increases with decreasing ring size [14].
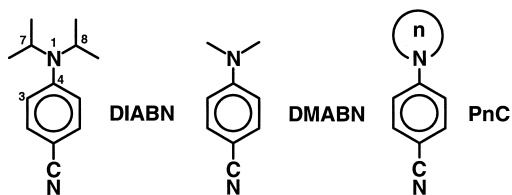
In tri(isopropyl)amine, the presence of three bulky isopropyl substituents results in a planarisation of the nitrogen atom [15,16], with a clearly smaller pyramidal angle than that present in trimethylamine [17] and triethylamine [15]. Based on our assumption that the decrease of the pyramidality of the amino nitrogen is an important reaction coordinate in the ICT reaction of dual fluorescent aminobenzonitriles [9,10,13], 4-(diisopropylamino)benzonitrile (DIABN) was synthesized. The photophysical behaviour of DIABN in *n*-hexane and isopentane solution, derived from photostationary and time-resolved measurements as a function of temperature, is presented here. It should be noted that with DMABN, dual fluorescence is not observed in alkane solvents such as *n*-hexane [8,18,19], even not at low temperatures, a condition under which an ICT emission is readily observed in the somewhat more polar solvents toluene and diethyl ether [4,9,10,20].

2. Experimental

DIABN (mp 81–84°C) was synthesised by bromination of N,N-diisopropylaniline (Aldrich), giving 4-bromo-N,N-diisopropylaniline [21], and subsequent replacement of the Br-substituent by CN in a reaction with CuCN [22]. DMABN was obtained from Aldrich. For both aminobenzonitriles, HPLC was the last purification step.

The solvents *n*-hexane and isopentane (Merck, Uvasol) were used as received. The other solvents employed in the solvatochromic measurements were chromatographed over Al_2O_3 just prior to use. The solutions, with an optical density between 0.4 and 0.6 for the maximum of the first band in the absorp-

tion spectrum, were deaerated by bubbling with nitrogen for 15 min.

The fluorescence spectra were measured with a quantum-corrected Shimadzu RF-5000PC. Fluorescence quantum yields Φ_f, with an estimated reproducibility of 2%, were determined with quinine sulfate in 1.0 N H_2SO_4 as a standard ($\Phi_f = 0.546$ at 25°C [23]).

The fluorescence decay times were determined with picosecond laser (excitation wavelength λ_{exc}, 276 or 297 nm) or nanosecond (λ_{exc}, 296 nm) flashlamp single-photon counting (SPC) setups. These setups and the analysis procedure of the fluorescence decays have been described previously [4,20]. The instrument response function has a half-width of 20–35 ps.

The yields Φ_{ISC} of the intersystem crossing from the equilibrated S_1 state to the lowest triplet state T_1 were measured by $T–T$ absorption, using a method based on triplet energy transfer with perylene as the acceptor [24,25]. As a reference substance N-methyl-1,8-naphthalimide was used, taking a value of 0.96 for Φ_{ISC} [26]. The solutions used in these experiments were degassed employing the freeze–pump–thaw method (5 cycles).

3. Results and discussion

3.1. Molecular structure of DIABN

The molecular structure of DIABN was determined by X-ray analysis [27]. The diisopropylamino group of DIABN (plane through C(7), N(1) and C(8)) is twisted over an angle of around 20° relative to the plane of the phenyl ring, different from the not-twisted dimethylamino group in DMABN [11]. The dihedral angle C(3)C(4)N(1)C(7) equals 24.3°, whereas an angle C(3)C(4)N(1)C(8) of 174.6° is found. The twist of the amino group in DIABN leads to a small lengthening of the N-phenyl bond N(1)–C(4) (1.38 Å) as compared with DMABN (1.37 Å) [11], but this bond remains clearly shorter than that of 3,5-dimethyl-4-(dimethylamino)benzonitrile (MMD), with an N(1)–C(4) bond length of 1.41 Å and an amino twist angle of 59° [11]. In accordance with these observations, the absorption spectrum of

DIABN is similar to that of DMABN (Fig. 1 and Section 3.4) and other 4-(dialkylamino)benzonitriles [5], but considerably different from that of MMD [19]. The pyramidality of the amino nitrogen N(1) in DIABN is slightly larger than in DMABN, as de-rived from the sum of the bond angles around N(1): 357.5° for DIABN and 358.8° [11] for DMABN.

3.2. Fluorescence spectra of DIABN and DMABN in n-hexane at 25°C

In the fluorescence spectrum of DMABN in *n*-hexane at room temperature only a single emission from the LE state is observed [18,19]. The occur-rence of dual fluorescence cannot be detected (see Fig. 1). DIABN in *n*-hexane at 25°C, in contrast, clearly is dual fluorescent. Its spectrum in Fig. 1 predominantly consists of an ICT emission (see Sec-tion 3.4) with a band maximum at around 26 000 cm^{-1}, strongly red-shifted with respect to the maxi-mum of the much weaker LE emission ($\sim$ 29 400 cm^{-1} (Table 1)). The ICT/LE fluorescence quan-tum yield ratio $\Phi'(ICT)/\Phi(LE)$ has a value of around 27 (Table 1), indicating that already at 25°C

the equilibrium of the ICT reaction is strongly shifted towards the ICT state [2].

3.3. Absorption spectra of DIABN and DMABN: $\Delta E(S_1,S_2)$

In the absorption spectrum of DMABN in *n*-hexane, the major S_2 band is clearly separated from the weaker structured S_1 band [19] (see Fig. 1). In the case of DIABN, the S_2 absorption band is red-shifted relative to that of DMABN, leading to a strongly reduced energy gap $\Delta E(S_1,S_2)$ for the for-mer molecule (Fig. 1). This observation is supported by linear dichroism measurements of DIABN and DMABN in stretched polyethylene films [28].

3.4. Solvatochromic measurements: ICT dipole mo-ment $\mu_e(ICT)$ of DIABN

To determine the dipole moment μ_e of the red-shifted main fluorescence band of DIABN (Fig. 1) and to verify its tentative identification given in Section 3.2. as coming from an ICT state, the ener-gies $\tilde{\nu}^{max}(flu)$ of the maxima of this emission band
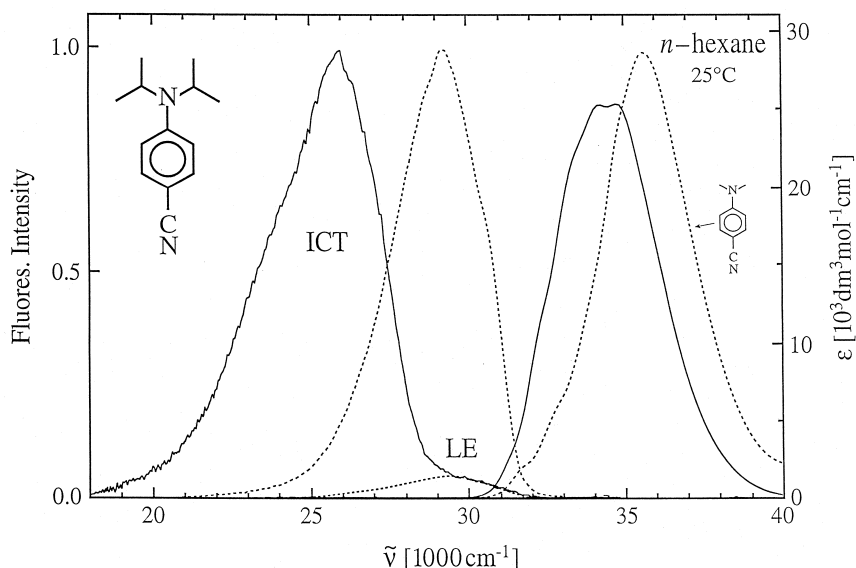

Fig. 1. Fluorescence and absorption spectra of (DIABN), full line, and 4-(dimethylamino)benzonitrile (DMABN), dashed line, in *n*-hexane at 25°C. The fluorescence of DIABN consists of emissions from an LE and an ICT state. Excitation wavelengths: 280 nm (DIABN) and 290 nm (DMABN).

Table 1

Energies $\tilde{\nu}^{\max}$ of the maximum of the ICT and the LE fluorescence bands and the absorption (abs) band of DIABN and DMABN in n-hexane (Fig. 1). The energy of the S_1 state $E(S_1)$, the extinction coefficient $\varepsilon^{\max}$ at $\tilde{\nu}^{\max}$(abs), the fluorescence quantum yields Φ'(ICT) and Φ(LE) of the ICT and LE states and the yield Φ_{ISC} of intersystem crossing are also listed

	T (°C)	$\tilde{\nu}^{\max}$(ICT) (1000 cm^{-1})	$\tilde{\nu}^{\max}$(LE) (1000 cm^{-1})	$\tilde{\nu}^{\max}$(abs) (1000 cm^{-1})	$E(S_1)^a$ (1000 cm^{-1})	$\varepsilon^{\max}$ (M^{-1}cm^{-1})	Φ'(ICT)	Φ(LE)	Φ'(ICT)/Φ(LE)	Φ_{ISC}
DIABN	25	26.05	($\sim$ 29.4)	34.1–34.8	31.2	25 560	0.008	$< 3.0 \times 10^{-4}$	> 27	0.94 ± 0.03[b]
DIABN	-90	25.6	29.2	–	–	–	0.005	$< 6.0 \times 10^{-4}$	> 7	(0.995)[c]
DMABN	25	–	29.3	35.5	31.7	28 860	0.0	0.18	0.0	0.76 ± 0.03[b]

[a] From crossing of absorption and fluorescence spectrum.

[b] From $T–T$ absorption (see text).

[c] From Φ'_{ISC}(ICT) $= k'_{ISC}$(ICT)·τ'_0(ICT) and τ'_0(ICT) $= k'_f$(ICT) + k'_{ISC}(ICT), under the assumption that internal conversion can be neglected (see data in Table 3 and text). Using the same procedure, a triplet yield Φ'_{ISC}(ICT) of 0.992 is obtained for DIABN in n-hexane at 25°C (see data in Table 3).

were measured at 25°C as a function of solvent polarity. These data are plotted in Fig. 2a against the polarity parameter $f{-}f'$ (Eqs. (1) and (2)) [29–31], as well as versus the ICT emission maxima $\tilde{\nu}^{max}(ICT)$ of DMABN obtained in the same solvents (see Fig. 2b).

$$\tilde{\nu}^{max}(flu) = \frac{-1}{4\pi\varepsilon_0} \frac{2}{hc\rho^3} \mu_e(\mu_e - \mu_g)(f-f')$$

$$+ \text{const.} \qquad (1)$$

where

$$f - f' = \frac{\varepsilon - 1}{2\varepsilon + 1} - \frac{n^2 - 1}{2n^2 + 1}. \qquad (2)$$

In Eq. (1), ρ is the equivalent spherical (Onsager) radius of the solute and ε_0 is the vacuum permittivity. The assumption is made that the dipole moment μ_g^{FC} of the Franck–Condon (FC) ground state reached upon emission from the relaxed S_1 state is identical with the ground state dipole moment $\mu_g(S_0)$ [31]. From the slope of the plot in Fig. 2a, proportional to $\mu_e(\mu_e - \mu_g)/\rho^3$ (Eq. (1)), a dipole moment μ_e of 16 ± 1 D is obtained (Table 2) by adopting for DIABN the μ_g value of 6.6 D measured for DMABN (supported by molecular mechanics calculations [32]). The radius ρ is calculated by taking the molecular density of DIABN to be equal to unity [31]. The scatter in the data points (Fig. 2a), generally observed in this solvatochromic procedure, can be reduced by plotting the $\tilde{\nu}^{max}(ICT)$ data of DIABN against the corresponding maxima of DMABN, thereby mutually compensating specific solute / solvent interactions.

The slope of this plot in Fig. 2b is equal to the expression $\mu_e(ICT)(\mu_e(ICT) - \mu_g(FC))/\rho^3$ (see Eq. (1)) for DIABN divided by that for DMABN. From the value of 0.85 ± 0.04 for this slope, an ICT dipole moment $\mu_e(ICT)$ of 18 ± 1 D is obtained for DIABN (Table 2), based on the dipole moment of 17 D for the ICT state of DMABN, which has been determined by the TRMC method [33]. A similar value for $\mu_e(ICT)$ was obtained for DMABN from an analysis of solvatochromic measurements [30]. The Onsager radius ρ of DMABN was again calculated by assuming a molecular density of 1.0. In this second method (Fig. 2b), the impact of ρ on the
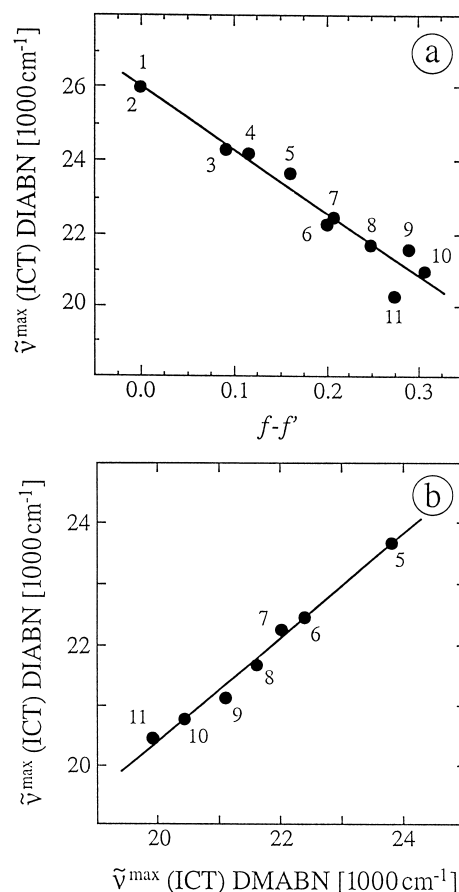

Fig. 2. Plots of the ICT emission maxima $\tilde{\nu}^{max}(ICT)$ of (DIABN) in a series of solvents at 25°C, against (a) the solvent polarity parameter $f-f'$ (Eq. (2)) and (b) the corresponding $\tilde{\nu}^{max}(ICT)$ data of 4-(dimethylamino)benzonitrile (DMABN). Solvents: (1) n-pentane, (2) n-hexane, (3) di(n-butyl) ether, (4) di(n-propyl) ether, (5) diethyl ether, (6) ethyl acetate, (7) tetrahydrofuran, (8) n-heptyl cyanide, (9) n-propyl cyanide, (10) acetonitrile, (11) N,N-dimethylformamide. Excitation wavelengths between 305 and 280 nm.

outcome of $\mu_e(ICT)$ obviously is much smaller than when the ratio $\mu_e(ICT)(\mu_e(ICT) - \mu_g)/\rho^3$ is used directly in the dipole moment determination (Fig. 2a). From the result now obtained for $\mu_e(ICT)$ of DIABN, it is concluded that the strongly Stokes-shifted main fluorescence band of DIABN in n-hexane (Fig. 1) indeed originates from an ICT state, with a similar dipole moment and hence intramolecular charge separation as that observed with DMABN.

Table 2

Dipole moment μ_e(ICT) of the ICT state and the activation energy E_a and the pre-exponential factor k_a^0 of the ICT reaction in *n*-hexane of DIABN

μ_e(ICT)[a] (D)	μ_e(ICT)[b] (D)	E_a [c] (kJ mol^{-1})	k_a^0 (10^{12} s^{-1})
18 ± 1	16 ± 1	5.7	3.5

  [a] Derived from the slope (0.85 ± 0.04) of the plot in Fig. 2b, with ρ(DIABN) = 4.31 Å and ρ(DMABN) = 3.87 Å (see Eq. (1).
  [b] Derived from the slope ($-17\,200 \pm 1300$ cm^{-1}) of the plot in Fig. 2a (see Eqs. (1) and (2).
  [c] See Fig. 5 and text.

3.5. Fluorescence quantum yields: influence of photoproducts

The total fluorescence quantum yield Φ_f of DIABN in *n*-hexane at 25°C, equal to the sum of the quantum yields Φ'(ICT) of the ICT and Φ(LE) of the LE emission, has a value of 0.008 (Table 1). It follows from the ratio Φ'(ICT)/Φ(LE) of around 27 (Table 1) that the LE fluorescence quantum yield is very small: 3×10^{-4}. Due to this small yield Φ(LE), the presence of even minor amounts of photoproducts complicates the accurate determination of Φ'(ICT)/Φ(LE). The value reported in Table 1 therefore is a lower limit.

With other 4-aminobenzonitriles, such a photodegradation is well-known. In the first publication on the dual fluorescence of DMABN, Lippert already pointed out that a photoproduct with a fluorescence spectrum similar to that of the LE emission is formed during irradiation [18].

3.6. Fluorescence spectra as a function of temperature

The fluorescence spectrum of DIABN in isopentane and *n*-hexane was measured as a function of temperature. The relative contribution of the LE emission to the dual fluorescence increases when the temperature is lowered (see Figs. 1 and 3). An influence of excitation wavelength (between 305 and 276 nm) on the fluorescence spectra was not observed. The observation that the ratio Φ'(ICT)/ Φ(LE) becomes smaller with decreasing temperature, indicates that DIABN is in the low-temperature limit, at which for the rate constant k_d of the ICT

$\rightarrow$ LE back reaction and the ICT lifetime τ_0' the condition $k_d \ll 1/\tau_0'$ holds [4], normally an indication of a large ICT reaction enthalpy $-\Delta H$ (see Section 3.9). From the slope of the Stevens–Ban plots (not shown) of $\ln(\Phi'(\text{ICT})/\Phi(\text{LE}))$ versus $1000\,T^{-1}$, equal to $-E_a/R$ [3,20], an ICT activation energy E_a for DIABN of 4 ± 1 kJ mol^{-1} in *n*-hexane and $k - d$ of 5.5 ± 0.5 kJ mol^{-1} in isopentane is obtained. Note that the appearance of structure in the ICT emission bands in Fig. 3 is not a common feature for aminobenzonitriles [1,2,4–10]. It is likewise observed with the strongly dipolar (21 D) fluorescence bands of electron donor/acceptor stilbenes such as 4-(dimethylamino)-4'-cyanostilbene (DCS)
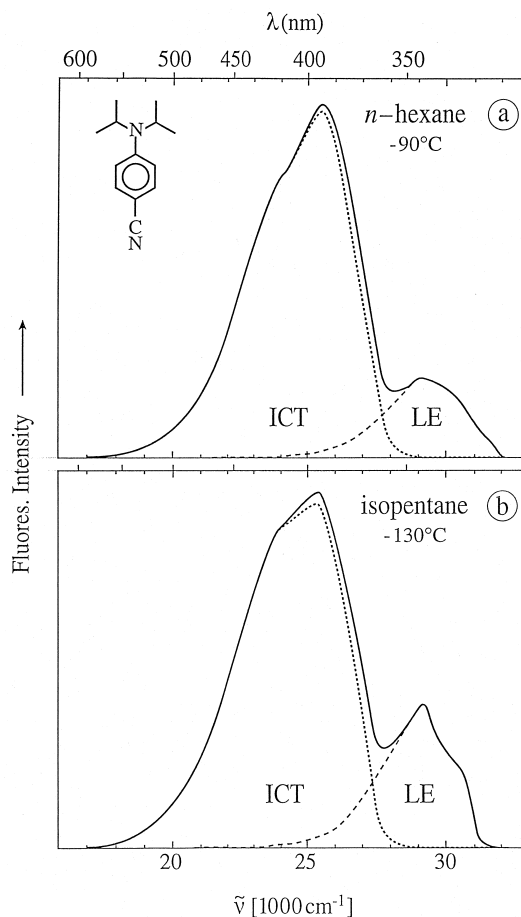

Fig. 3. Fluorescence spectra of DIABN in (a) *n*-hexane at -90°C and (b) isopentane at -130°C. The separate emissions from the LE and ICT states are shown. Excitation wavelength: 280 nm.

in alkane solvents [31]. As well for DIABN and the other dual fluorescent 4-aminobenzonitriles as for DCS, structureless and symmetric emission bands are found in solvents more polar than alkanes [4,8,31].

3.7. Intersystem crossing yields at 25°C: no internal conversion

For DIABN in *n*-hexane at 25°C a triplet yield Φ_{ISC} of 0.94 ± 0.03 is determined. The sum of Φ_{ISC} and the total fluorescence quantum yield Φ_f does not deviate appreciably from unity (0.95 ± 0.03 (Table 1)). It hence follows that internal conversion (IC) is not an important deactivation pathway for DIABN
in *n*-hexane at room temperature.

3.8. LE and ICT fluorescence decays in n-hexane at −90°C

A global analysis [4] of the fluorescence decays $i_f(LE)$ and $i_f(ICT)$ of DIABN in *n*-hexane at −90°C

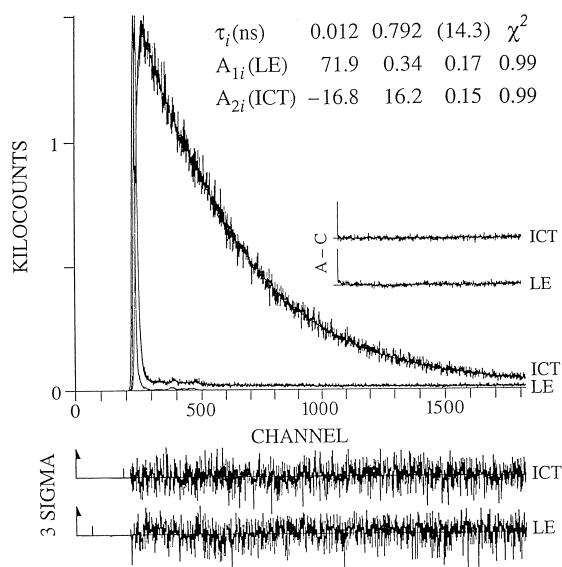| τ_i(ns)	0.012	0.792	(14.3)	χ^2
A_{1i}(LE)	71.9	0.34	0.17	0.99
A_{2i}(ICT)	−16.8	16.2	0.15	0.99

Fig. 4. LE and ICT fluorescence response functions of DIABN in *n*-hexane at −90°C. The LE and ICT decays are analysed simultaneously (global analysis). The decay times (τ_2, τ_1) and their pre-exponential factors A_{1i} and A_{2i} are given (Eqs. (3) and (4)). The shortest decay time τ_2 is listed first. The time in parentheses is attributed to a photoproduct (see text). The weighted deviations, expressed in σ (expected deviations), the autocorrelation functions $A-C$, and the values for χ^2 are also indicated. Excitation wavelength: 297 nm.

is shown in Fig. 4. The decays are made up of two exponentials, both with a short decay time τ_2 of 12 ps and a longer time τ_1 of 0.79 ns. The third decay time of 14.3 ns appearing in the two decays is attributed to a photoproduct, as its contribution to the total fluorescence decay increases with the duration of the laser excitation (Section 3.5).

$$i_f(LE) = A_{11}\exp(-t/\tau_1) + A_{12}\exp(-t/\tau_2),$$

(3)

$$i_f(ICT) = A_{21}\exp(-t/\tau_1) + A_{22}\exp(-t/\tau_2),$$

(4)

$$A = A_{12}/A_{11}.$$

(5)

From the decay times τ_2 and τ_1 together with the amplitude ratio A (Eqs. (3) and (5)) and the model compound lifetime τ_0, the ICT rate constants k_a and k_d and the lifetime $\tau'_0(ICT)$ can be determined [4,20] (see Table 3). The fluorescence lifetime of DMABN in *n*-hexane was taken for τ_0, as dual emission is not observed with this system (Fig. 1). The radiative rate constants $k_f(LE)$ and $k'_f(ICT)$ can be determined from the fluorescence quantum yields $\Phi(LE)$ and $\Phi'(ICT)$ (see Tables 1 and 3). The observation that the amplitude ratio A_{22}/A_{21} (Eq. (4)) is equal to −1.0 (see Fig. 4), shows that the ICT state of DIABN is not formed by direct excitation from the ground state, but originates exclusively from the primarily formed LE state [4,5,20].

3.8.1. k_a, $\tau'_0(ICT)$ and $k'_{ISC}(ICT)$

For the ICT reaction of DIABN in *n*-hexane at −90°C, a rate constant k_a of 8×10^{10} s^{-1} is obtained. The lifetime $\tau'_0(ICT)$ equals 0.79 ns. As there is no evidence for appreciable internal conversion from the ICT state (Section 3.7.), only fluorescence and ISC deactivate the ICT state and $1/\tau'_0(ICT) = k'_{ISC}(ICT) + k'_f(ICT)$. From the data in Table 3, it is seen that $k'_f(ICT)$ can be neglected with respect to $k'_{ISC}(ICT)$: $1/\tau'_0(ICT) = k'_{ISC}(ICT)$. This leads to $k'_{ISC}(ICT)$ values of 1.27 and 1.06×10^9 s^{-1} at −90 and 25°C, respectively. Using these data, it follows from $\Phi'_{ISC}(ICT) = k'_{ISC}(ICT) \cdot \tau'_0(ICT)$ that the triplet yield from the ICT state $\Phi'_{ISC}(ICT)$ amounts to 0.995 at −90°C and 0.992 at 25°C (see Table 1). These

Table 3
Fluorescence decay times τ_2 and τ_1 (Eqs. (3) and (4)) and τ_0, amplitude ratio A (Eq. (5)), rate constants of the forward (k_a) and backward (k_d) ICT reactions, ICT fluorescence lifetime $\tau'_0(ICT)$, the LE and ICT radiative rate constants $k_f(LE)$ and $k'_f(ICT)$ and the rate constant $k'_{ISC}(ICT)$ of the intersystem crossing (ISC) from the ICT state

T (°C)	τ_2 (ns)	τ_1 (ns)	A	τ_0 (ns)	k_a (10^{11} s^{-1})	k_d (10^8 s^{-1})	$\tau'_0(ICT)$ (ns)	$k_f(LE)$ (10^7 s^{-1})	$k'_f(ICT)$ (10^6 s^{-1})	$k'_f(ICT)k_f(LE)$	$k'_{ISC}(ICT)$ (10^9 s^{-1})
25.5	0.003	0.94	> 430	3.42[a]	3.4[b]	< 8	0.94	6[c]	9[d]	0.17[e]	1.0[f]
−90.3	0.012	0.79	> 210	4.10[a]	0.8	< 4	0.79	4[c]	6[d]	0.15[e]	1.3[g]

[a] Fluorescence decay time τ_0 of DMABN in n-hexane.
[b] From data in Fig. 5 (see Fig. 4).
[c] From $\Phi(LE)$ (see Table 1 and the expression $k_f = \Phi(LE)(1/\tau_0 + 1/\tau'_0 \cdot k_a /(k_d + 1/\tau'_0))$ (see text).
[d] From $\Phi'(ICT)$ (see Table 1) and the expression $k'_f = \Phi'(ICT)(1/\tau'_0 + 1/\tau_0 \cdot (k_d + 1/\tau'_0)/k_a)$ (see text).
[e] From the data for $\Phi'(ICT)/\Phi(LE)$ in Table 1 and the expression (Ref. [4]) $\Phi'(ICT)/\Phi(LE) = k'_f(ICT)/k_f(LE) \cdot k_a /(k_d + 1/\tau'_0(ICT))$.
[f] From $k'_{ISC} = \Phi'(ISC)/\tau'_0(ICT)$ (see Table 1).
[g] From $k'_{ISC}(ICT) = 1/\tau'_0(ICT) - k'_f(ICT)$, under the assumption that internal conversion can be neglected (see data in this table and text (Section 3.7).

results show that ISC is the predominant deactivation pathway of the ICT state.

3.8.2. A and k_d

The amplitude ratio $A = A_{12}/A_{11}$ (Eq. (5)) has at $-90°C$ a value of 210 (Table 3), which is a lower limit due to the presence of photoproducts (Section 3.5). As A is approximately equal to k_a/k_d under the present conditions [4,20], this means that the rate constant of the forward ICT reaction k_a is at least 210 times larger than the thermal back reaction k_d, i.e., k_d is smaller than 4×10^8 s^{-1}. It should be noted in this connection, that the LE fluorescence quantum yield Φ_{LE} of DIABN in n-hexane at $-90°C$ is very small: 6×10^{-4} (Table 1). As a consequence, minor amounts of photoproducts or other impurities (Section 3.5) with fluorescence decay times in the nanosecond time range [4,18,20] will lead to a decrease of the amplitude ratio A. The value obtained here for k_d from A and τ_2 (Table 3) therefore is an upper limit. It cannot be excluded that k_d for DIABN in n-hexane at $-90°C$ is in fact equal to zero.

3.9. Fluorescence decays as a function of temperature: DIABN in n-hexane

The fluorescence decay of DIABN in n-hexane was measured as a function of temperature. Identical results were obtained at the two excitation wavelengths 297 and 276 nm. The short decay time τ_2 decreases with increasing temperature, from 12 ps at $-90°C$ (Fig. 4) to 3 ps at 25°C (see Fig. 5). As τ_2 is practically equal to the reciprocal of the ICT rate constant k_a under the prevailing experimental conditions ($\tau_2 << \tau_1$ [4,20]), the activation energy E_a can be obtained from an Arrhenius plot of τ_2. From the line fitting the data points in Fig. 5, an energy E_a of 6 kJ mol^{-1} and a pre-exponential factor k_a^o of 3.5×10^{12} s^{-1} result (Table 2), in agreement with the approximate value of 4 ± 1 kJ mol^{-1} determined from a Stevens–Ban plot (Section 3.6). The activation energy E_d of the ICT → LE rate constant k_d and hence the ICT stabilisation enthalpy ΔH cannot be determined with sufficient accuracy, because of the uncertainty in the amplitude ratio A (Section 3.8).

With DMABN in toluene, an activation energy E_a of 8 kJ mol^{-1} has been determined [4] and E_a
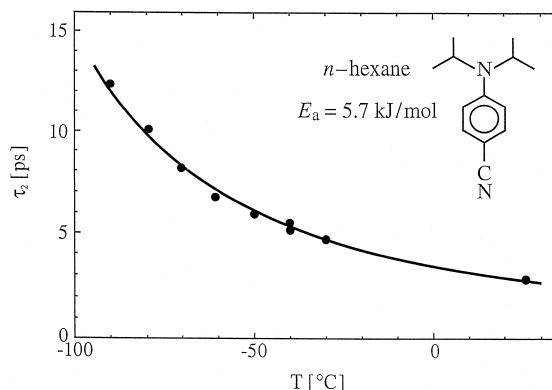

Fig. 5. Plot of the short fluorescence decay time τ_2 of DIABN in n-hexane as a function of temperature. The line through the data points represents a least-squares fit, resulting in an ICT activation energy E_a of 5.7 kJ mol^{-1} and a pre-exponential factor k_a^0 of 3.5×10^{12} s^{-1} (see text). Excitation wavelengths: 276 and 297 nm.

becomes larger when the solvent polarity decreases [34], from 5 kJ mol^{-1} in diethyl ether up to 20 kJ mol^{-1} in di(n-pentyl) ether [35]. For the nonpolar solvent n-hexane a still higher barrier is expected. It is therefore concluded that the absence of dual fluorescence with DMABN in n-hexane is, apart from an unfavourable (probably positive) ΔH [19,31,35], caused by the fact that its ICT activation energy is considerably larger than that of DIABN.

4. Conclusions

With DIABN, efficient ICT and dual fluorescence is observed in nonpolar alkane solvents such as n-hexane and isopentane, from room temperature down to -90 or $-130°C$, respectively, in clear contrast to what is found with DMABN. The fluorescence spectrum of DIABN in these alkanes predominantly consists of an emission from the ICT state, with a $\Phi'(ICT)/\Phi(LE)$ ratio of around 27 in n-hexane at 25°C. An ICT dipole moment $\mu_e(ICT)$ of 18 D is obtained for DIABN from solvatochromic measurements, similar to that of DMABN.

From an analysis of LE and ICT fluorescence decays it is found that with DIABN a fast ICT reaction occurs, with a rate constant k_a of 3.4×10^{11} s^{-1} at 25°C in n-hexane, slowing down somewhat to

8×10^{10} s^{-1} at $-90°C$. This reaction has an activation energy E_a of 6 kJ mol^{-1}. Efficient ISC, with a yield Φ_{ISC} of 0.94 at 25°C, takes place from the ICT state.

The occurrence of fast ICT with DIABN in alkane solvents such as *n*-hexane and isopentane mainly results from the considerably smaller energy gap $\Delta E(S_1, S_2)$ of DIABN as compared with DMABN, which leads to a decrease in the activation energy E_a of the ICT reaction, in support of the PICT model [2,4,9,10]. With DIABN and DMABN the ICT activation energy E_a is not predominantly determined by the change in pyramidality of the amino nitrogen N(1), in contrast to what has been observed [9,10,13] with 4-(azetidinyl)benzonitrile (P4C).

Acknowledgements

References

[1] W. Rettig, B. Bliss, K. Dirnberger, Chem. Phys. Lett. 305 (1999) 8.

[2] K.A. Zachariasse, Chem. Phys. Lett. 320 (2000) 8.

[3] C. Chudoba, A. Kummrow, J. Dreyer, J. Stenger, E.T.J. Nibbering, T. Elsaesser, K.A. Zachariasse, Chem. Phys. Lett. 309 (1999) 357.

[4] Yu.V. Il'ichev, W. Kühnle, K.A. Zachariasse, J. Phys. Chem. 102 (1998) 5670.

[5] K.A. Zachariasse, M. Grobys, E. Tauer, Chem. Phys. Lett. 274 (1997) 372.

[6] W. Rettig, in: J. Mattay (Ed.), Topics in Current Chemistry, Electron Transfer I, vol. 169, Springer, Berlin, 1994, p. 253.

[7] Z.R. Grabowski, K. Rotkiewicz, A. Siemiarczuk, D.J. Cowley, W. Baumann, Nouv. J. Chim. 3 (1979) 443.

[8] W. Rettig, Angew. Chem. Int. Ed. Engl. 25 (1986) 971.

[9] K.A. Zachariasse, M. Grobys, Th. von der Haar, A. Hebecker, Yu.V. Il'ichev, Y.-B. Jiang, O. Morawski, W. Kühnle, J. Photochem. Photobiol. A: Chem. 102 (1996) 59.

[10] K.A. Zachariasse, M. Grobys, Th. von der Haar, A. Hebecker, Yu.V. Il'ichev, O. Morawski, I. Rückert, W. Kühnle, J. Photochem. Photobiol. A: Chem. 105 (1997) 373.

[11] A. Heine, R. Herbst-Irmer, D. Stalke, W. Kühnle, K.A. Zachariasse, Acta Cryst. B 50 (1994) 363.

[12] G. Berden, J. van Rooy, W.L. Meerts, K.A. Zachariasse, Chem. Phys. Lett. 278 (1997) 373.

[13] Th. von der Haar, A. Hebecker, Yu.V. Il'ichev, Y.-B. Jiang, W. Kühnle, K.A. Zachariasse, Recl. Trav. Chim. Pays-Bas 114 (1995) 430.

[14] M. Oki, Applications of Dynamic NMR Spectroscopy to Organic Chemistry, VCH, Weinheim, 1985.

[15] R. Boese, D. Bläser, M.Y. Antipin, V. Chaplinski, A. de Meijere, J. Chem. Soc., Chem. Commun., 1998, p. 781.

[16] H. Bock, I. Göbel, Z. Havlas, S. Liedle, H. Oberhammer, Angew. Chem. Int. Ed. Engl. 30 (1991) 187.

[17] A.J. Blake, E.A.V. Ebsworth, A.J. Welch, Acta Cryst. C 40 (1984) 413.

[18] E. Lippert, W. Lüder, F. Moll, W. Nägele, H. Boos, H. Prigge, I. Seibold-Blankenstein, Angew. Chem. 73 (1961) 695.

[19] K.A. Zachariasse, Th. von der Haar, A. Hebecker, U. Leinhos, W. Kühnle, Pure Appl. Chem. 65 (1993) 1745.

[20] U. Leinhos, W. Kühnle, K.A. Zachariasse, J. Phys. Chem. 95 (1991) 2013.

[21] R. Reynaud, Bull. Soc. Chim. Fr., 1967, p. 2686.

[22] S.-D. Yoh, Y. Tsuno, M. Fujio, M. Sawada, Y. Yukawa, J. Chem. Soc. Perkin Trans. 2 (1989) 7.

[23] J.N. Demas, G.A. Crosby, J. Phys. Chem. 75 (1971) 991.

[24] I. Carmichael, W.P. Helman, G.L. Hug, J. Phys. Chem. Ref. Data 16 (1987) 239.

[25] L. Biczok, T. Berces, H. Inoue, J. Phys. Chem. A 103 (1999) 3837.

[26] A. Demeter, S. Braslavski, unpublished results.

[27] M. Noltemeyer, K.A. Zachariasse, in preparation.

[28] T. Thormann, P.W. Thulstrup, K.A. Zachariasse, unpublished results.

[29] W. Liptay, in: E.C. Lim (Ed.), Excited states, vol. 1, Academic Press, New York, 1974, p. 129.

[30] W. Baumann, H. Bischof, J.-C. Brittinger, W. Rettig, K. Rotkiewicz, J. Photochem. Photobiol. A: Chem. 64 (1992) 49.

[31] Yu.V. Il'ichev, W. Kühnle, K.A. Zachariasse, Chem. Phys. 211 (1996) 441.

[32] J.J. Gajewski, K.E. Gilbert, L. McKelvey, in: D. Liotta (Ed.), Advances in Molecular Modelling, vol. II, JAI Press, Greenwich, CN, 1990, p. 65.

[33] W. Schuddeboom, S.A. Jonker, J.M. Warman, U. Leinhos, W. Kühnle, K.A. Zachariasse, J. Phys. Chem. 96 (1992) 10809.

[34] J.M. Hicks, M.T. Vandersall, E.V. Sitzmann, K.B. Eisenthal, Chem. Phys. Lett. 135 (1987) 413.

[35] U. Leinhos, Ph.D. Thesis, University Göttingen 1991.